THE JOURNAL OF BIOLOGICAL CHEMISTRY
Vol. 276, No. 29, Issue of July 20, pp. 27400–27405, 2001
© 2001 by The American Society for Biochemistry and Molecular Biology, Inc.
Printed in U.S.A.

Rapid Activation of Transducin by Mutations Distant from the Nucleotide-binding Site

EVIDENCE FOR A MECHANISTIC MODEL OF RECEPTOR-CATALYZED NUCLEOTIDE EXCHANGE BY G PROTEINS*

Received for publication, April 17, 2001, and in revised form, May 9, 2001
Published, JBC Papers in Press, May 16, 2001, DOI 10.1074/jbc.C100198200

Ethan P. Marin‡, A. Gopala Krishna‡§, and Thomas P. Sakmar‡§¶

From the §Howard Hughes Medical Institute and the ‡Laboratory of Molecular Biology and Biochemistry, The Rockefeller University, New York, New York 10021

G proteins act as molecular switches in which information flow depends on whether the bound nucleotide is GDP ("off") or GTP ("on"). We studied the basal and receptor-catalyzed nucleotide exchange rates of site-directed mutants of the α subunit of transducin. We identified three amino acid residues (Thr-325, Val-328, and Phe-332) in which mutation resulted in dramatic increases (up to 165-fold) in basal nucleotide exchange rates in addition to enhanced receptor-catalyzed nucleotide exchange rates. These three residues are located on the inward facing surface of the α5 helix, which lies between the carboxyl-terminal tail and a loop contacting the nucleotide-binding pocket. Mutation of amino acid residues on the outward facing surface of the same α5 helix caused a decrease in receptor-catalyzed nucleotide exchange. We propose that the α5 helix comprises a functional microdomain in G proteins that affects basal nucleotide release rates and mediates receptor-catalyzed nucleotide exchange at a distance from the nucleotide-binding pocket.

G protein[1]-coupled receptors (GPCRs) activate G proteins by catalyzing the release of GDP bound to the G protein α subunit (Gα) (1–3). GTP-bound Gα proteins regulate a variety of cellular effector enzymes or ion channels. The active Gα is turned off kinetically by intrinsic GTPase activity, which is highly regulated by bound effector and regulator of G protein signaling proteins (4, 5). High resolution structural analysis of several nucleotide-bound forms of Gα (6–9) and of complexes of Gα subunits with regulatory proteins (10, 11) have provided insights into key conformational changes required for G protein function. In addition, the crystal structure of rhodopsin (12), a prototypical GPCR, provides a basis for understanding several key features of the molecular physiology of rhodopsin (13). However, structural information is lacking for the receptor-bound nucleotide-free conformation of Gα, and the molecular details of how GPCRs switch G proteins from their inactive to active states remains unknown. Interestingly, the receptor must act at a distance because extensive evidence from biochemical and mutagenesis work suggests that the cytoplasmic loops of the active receptor (R*) do not directly contact the nucleotide-binding pocket of Gα subunits (14).

To address the question of how GPCRs catalyze the switching of GDP for GTP by G proteins, we studied the mechanism of nucleotide exchange in transducin (Gα_t). We chose to study Gα_t because it exhibits an extremely low basal GDP release rate (15) and a very rapid R*-catalyzed nucleotide exchange rate (16) consistent with its role in rod cell visual phototransduction where low biochemical noise levels are required. We tested the hypothesis that the α5 helix of Gα_t is one of the structural features that resolves the action at a distance problem and explains how R* induces nucleotide switching by G proteins (17, 18). The α5 helix of Gα_t (amino acid residues 325–339) connects the carboxyl-terminal tail of Gα_t to the β6/α5 loop. The carboxyl tail of Gα_t, especially amino acid residues 340–350, is a well characterized binding domain for R* (19–23), and the β6/α5 loop directly contacts the guanine ring of the bound nucleotide. Consequently, R* might induce nucleotide exchange in Gα_t by using the α5 helix to communicate between the carboxyl terminus and the β6/α5 loop.

We report that mutation of several specific residues on the buried surface of α5 caused dramatic increases in the basal nucleotide exchange rates in the resulting Gα_t mutants. The evidence suggests that the mechanism of R*-catalyzed nucleotide exchange by Gα_t involves conformational changes in these α5 residues. R* may induce changes in α5 either directly by binding to α5 or indirectly by binding to the adjacent carboxyl terminus. We propose that the α5 helix controls the basal nucleotide exchange rate and mechanistically couples R* binding to the guanine nucleotide in Gα_t.

EXPERIMENTAL PROCEDURES

Most of the methods used in this paper have been described previously (24). Brief descriptions are given below.

Site-directed Mutagenesis of Gα_t and Expression in Vitro—Site-directed mutations were created using the QuickChange system (Stratagene). The parent for all Gα_t constructs was pGEM2sTα, the synthetic bovine Gα_t gene cloned into the pGEM2 plasmid under the control of a SP6 promoter (25). Gα_t and Gα_t mutant proteins were prepared *in vitro* using the TnT Quick Coupled transcription/translation system (Promega). The translated products were passed over BioSpin 6 gel filtration spin columns (Bio-Rad) twice consecutively to remove excess nucleotides and [^{35}S]methionine. The volume of each sample was then adjusted to 100 μl in Buffer A (5 mM Tris-HCl, pH 7.5, 150 mM NaCl, 2 mM $MgCl_2$, 1 mM dithiothreitol, 0.01% (w/v) *n*-dodecyl-β-D-maltoside). If the sample was to be studied in a R*-catalyzed assay, G$\beta\gamma_t$ was added to a final concentration of 30 nM. Every experiment was performed using freshly translated material.

* This research was supported in part by the Allene Reuss Memorial Trust and National Institutes of Health Training Grants GM07739 and GM07982. The costs of publication of this article were defrayed in part by the payment of page charges. This article must therefore be hereby marked "*advertisement*" in accordance with 18 U.S.C. Section 1734 solely to indicate this fact.

¶ Associate Investigator of the Howard Hughes Medical Institute. To whom correspondence should be addressed: Rockefeller University, 1230 York Ave., New York, NY 10021. Tel.: 212-327-8288; Fax: 212-327-7904; E-mail: sakmar@rockvax.rockefeller.edu.

[1] The abbreviations used are: G protein, guanine nucleotide-binding regulatory protein; Gα_t, α subunit of transducin; G$\beta\gamma_t$, $\beta\gamma$ subunits of transducin; GPCR, G protein-coupled receptor; R*, signaling active conformation of rhodopsin; GTPγS, guanosine 5′-*O*-(thiotriphosphate).

This is an open access article under the CC BY license.

This paper is available on line at http://www.jbc.org

Nucleotide Exchange Rate Assays—Samples (70 μl each) of translated $G\alpha_t$ or mutant $G\alpha_t$ kept on ice in Buffer A were quickly warmed to room temperature in a water bath. For basal exchange rate assays (Fig. 1), the experiment was initiated by the addition of GTPγS to a final concentration of 100 μM. Five aliquots (8 μl) were withdrawn during a period ranging from 2 to 6 h and digested. For R*-catalyzed assays (Fig. 2), the experiment was initiated by the addition of a mixture of R* and GTPγS (4 μl) to a final concentration of 30 nM R* and 14 μM GTPγS. Immediately before addition to the reaction, the rhodopsin was photolyzed by illumination for 15 s with a fiber optic cable connected to a Dolan Jenner lamp equipped with a >495-nm long pass filter. The samples were incubated at room temperature under illumination. Aliquots (8 μl) were withdrawn and digested at 1, 2, 3, 5, 10, and 20 min. The digestion procedure was adapted from Garcia *et al.* (20). Aliquots were mixed with 1.5 μl of digest buffer (5% Lubrol, 2 mM GDP, 1 mg/ml L-1-tosylamido-2-phenylethyl chloromethyl ketone-treated trypsin) and incubated on ice for 30 min. Digestion was terminated by the addition of 2.5 μl of termination solution (10 mg/ml aprotinin, 10 μM phenylmethylsulfonyl fluoride), followed by 6 μl of 3× SDS sample buffer (New England Biolabs). The proteolytic fragments were resolved by SDS-polyacrylamide gel electrophoresis using precast 15% gels (Bio-Rad). The intensities of the fragments were quantitated by phosphorimaging using a Storm Imager and ImageQuant software (Molecular Dynamics). $G\alpha_t$ in the GDP-bound inactive conformation yielded an ~23-kDa fragment, and $G\alpha_t$ in the active conformation (GTPγS- or GDP-AlF_4^--bound) yielded an ~34-kDa fragment following trypsin digestion. The fraction of $G\alpha_t$ activated in a given sample was determined from the relative intensity of the two bands. The ~23-kDa bands were generally absent from digests of the F185A and F192A mutants of $G\alpha_t$ (not shown), although they could bind GDP as indicated by activation by AlF_4^- and the rate of GTP uptake. Instead, the mutations seemed to affect the folding or stability of the proteins. The rates of nucleotide exchange in F185A and F192A could be estimated from the intensities of the ~34-kDa bands.

RESULTS AND DISCUSSION

We carried out alanine-scanning mutagenesis of the 14 non-alanine amino acid residues in the α5 helix of $G\alpha_t$. Proteins were expressed *in vitro* in rabbit reticulocyte lysate to overcome the well documented problems with the heterologous expression of $G\alpha_t$ (26, 27). Nucleotide exchange rates were determined using a quantitative trypsin digest assay specifically adapted for kinetic measurements. The assay is directly sensitive to the nucleotide-bound status of $G\alpha_t$ (28) and does not rely on potentially confounding second messenger readouts. The sensitivity and fidelity of this assay has been described in detail (24).

Three of the fourteen mutants (T325A, V328A, and F332A) exhibited tremendous increases in their rates of basal nucleotide exchange (Fig. 1, *A* and *B*; Table I). The basal exchange rates of V328A, F332A, and T325A were accelerated by 77-, 151-, and 165-fold, respectively, over the basal exchange rate of wild-type $G\alpha_t$ measured under the identical conditions. These rates are comparable with or in excess of the basal exchange rate of mutant A322S (63-fold increase) (Fig. 1, *A* and *B*; Table I). Ala-322 is known to reside in the β6/α5 loop and to be in contact with GDP. The A322S mutant is also analogous to mutations in $G\alpha_s$ and $G\alpha_i$ that have been reported to greatly increase the basal nucleotide exchange rates (29, 30). These results suggest that alteration of the α5 helix, which is distant from the nucleotide, can accelerate GDP release to an even greater degree than replacement of amino acids known to be in direct contact with the nucleotide.

The mutants N327A and I339A also exhibited statistically significant gain of function phenotypes (Table I). Together, the five residues that displayed an increase in basal nucleotide exchange rate are found to be clustered along the buried surface of the α5 helix (Fig. 3). Thr-325 is located in the first turn of the α5 helix, immediately adjacent to the β6/α5 loop. Asn-327 is also located on the first turn, a structure that appears to be stabilized by a network of hydrogen bonds. Substitution of the amino acid side chains in this region might be expected to disrupt some of these hydrogen bonds and alter the structure of the first turn and possibly the β6/α5 loop. Two other residues, Val-328 and Phe-332, point in toward the center of $G\alpha_t$ and contribute to its hydrophobic core. Val-328 and Phe-332 make extensive contacts with residues from the α1 helix, as well as the β2 and β3 sheets. Loops emanating from these structural elements contribute to the canonical nucleotide-binding surfaces of $G\alpha_t$ and other G proteins (31). Replacement of Val-328 or Phe-332 with alanine is likely to perturb the packing of the β2 and β3 sheets and the α1 helix in a manner that affects the structure of the nucleotide-binding pocket.

All of the alanine replacement mutants, including V328A,

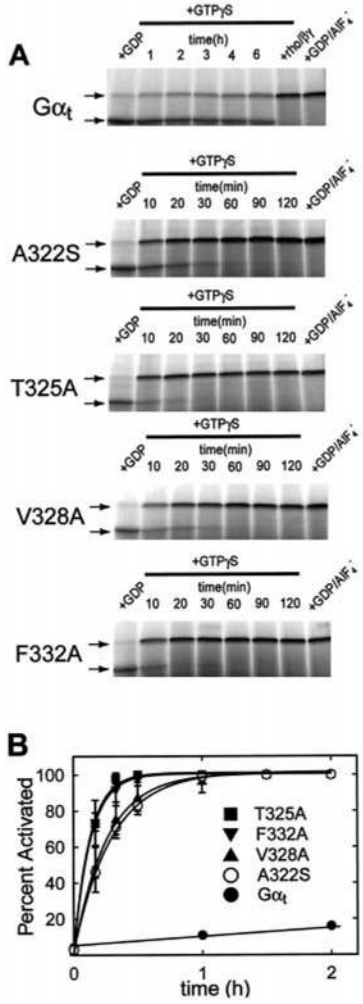

FIG. 1. **Basal nucleotide exchange rates of $G\alpha_t$ and $G\alpha_t$ mutants determined by quantitative trypsin digests.** *A*, trypsin digest reactions of $G\alpha_t$ and $G\alpha_t$ mutants that display accelerated basal nucleotide exchange rates. $G\alpha_t$ was expressed *in vitro* in the presence of [^{35}S]methionine and digested with trypsin following treatment with 100 μM GDP, 100 μM GTPγS, or 100 μM GDP,170 μM $AlCl_3$,10 mM NaF. The resulting fragments were resolved by SDS-polyacrylamide gel electrophoresis and visualized by phosphorimaging. *Arrows* indicate the position of ~34- and ~23-kDa bands. The fraction of $G\alpha_t$ bound to GTPγS or GDP was determined from the relative intensity of the ~34-kDa band (which corresponds to activated $G\alpha_t$) to the ~23-kDa band (which corresponds to inactive $G\alpha_t$). The basal rate of nucleotide exchange was determined by examining aliquots taken at indicated times following addition of GTPγS (100 μM). All the mutants folded properly and could bind GDP, GTPγS, and AlF_4^- as indicated by the trypsin digest pattern. *B*, basal nucleotide exchange time course derived from trypsin digest analysis. The mutants T325A, V328A, and F332A all displayed extremely fast nucleotide exchange kinetics that exceeded the rate of A322S, a mutation of a nucleotide-contacting residue. Data points represent the mean of at least three independent experiments; *error bars* depict ±2 × S.E. *Solid lines* are fits to the equation: $y = c + 100(1 - \exp(-k_{app}t))$.

TABLE I
Apparent rate constants for nucleotide exchange measured for $G\alpha_t$ and $G\alpha_t$ mutants

Mutant	Basal	
	k_{app}[a]	-Fold increase[b]
Wild-type	8.6 ± 0.7	1.0 ± 0.1
Q168A	26.4 ± 5.2	3.1 ± 0.7
F187A	4.8 ± 0.8	0.6 ± 0.1
K188A	48.5 ± 13.1	5.7 ± 1.6
A322S	536 ± 109	62.6 ± 13.7
T325A	1410 ± 474	165 ± 57
Q326A	6.6 ± 1.3	0.8 ± 0.2
N327A	198 ± 60	23 ± 7.2
V328A	661 ± 185	77 ± 23
K329A	9.0 ± 0.9	1.0 ± 0.1
F330A	5.3 ± 1.2	0.6 ± 0.1
V331A	9.6 ± 2.0	1.1 ± 0.3
F332A	1300 ± 256	151 ± 32
D333A	6.4 ± 0.3	0.7 ± 0.1
V335A	17.7 ± 2.2	2.1 ± 0.3
T336A	7.4 ± 2.0	0.9 ± 0.2
D337A	17.3 ± 4.2	2.0 ± 0.5
I338A	9.3 ± 1.1	1.1 ± 0.2
I339A	35.4 ± 23	4.1 ± 2.7

[a] The apparent rate constants for basal nucleotide exchange were derived from fits of each data set to the exponential rise equation, $y = c + 100(1 - \exp(-k_{app}t))$. Each mutant protein was assayed at least 3 times (wild-type $G\alpha_t$ protein was assayed 26 times), and an independent fit was made to each data set. The values reported are the mean $k_{app} \times 10^4$ $min^{-1} \pm 2 \times$ S.E.

[b] The -fold increase in the nucleotide exchange rate measured for the mutant protein relative to that of uncatalyzed wild-type $G\alpha_t$ was calculated as the k_{app}(mutant)/k_{app}(wild-type).

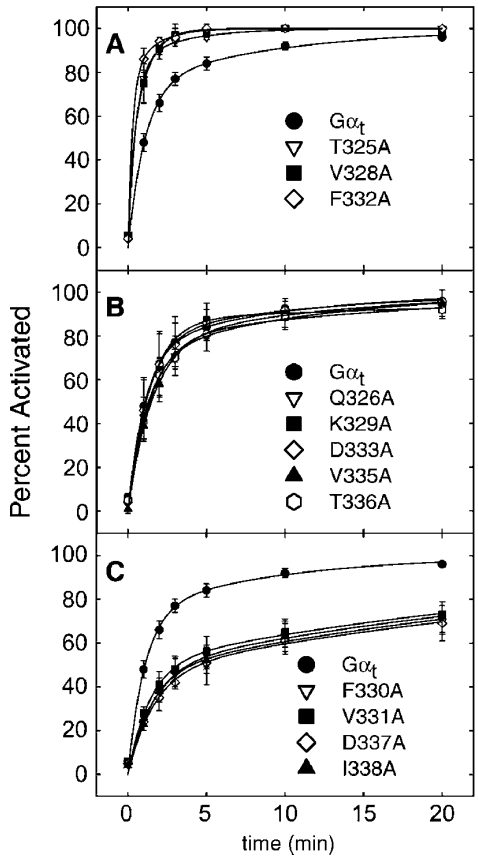

FIG. 2. **R*-catalyzed nucleotide exchange time course derived from trypsin digest analysis.** Translated $G\alpha_t$ was combined with 30 nM $G\beta\gamma_t$, 30 nM photoactivated rhodopsin, and 14 μM GTPγS; aliquots were removed at the indicated times and analyzed. Data points represent the mean of at least three independent experiments; *error bars* depict $\pm 2 \times$ S.E. Values for the $t_{1/2}$ of nucleotide exchange (in minutes) were estimated from double exponential fits of the data (*solid lines*). The $t_{1/2}$ for wild-type $G\alpha_t$ was 1.1. *A*, the mutants that displayed highly accelerated basal nucleotide exchange rates also displayed accelerated R*-catalyzed nucleotide exchange. The estimated values for $t_{1/2}$ were: T325A, 0.4; V328A, 0.4; F332A, 0.2. *B*, five mutants were indistinguishable from wild-type $G\alpha_t$. The estimated values for $t_{1/2}$ were: Q326A, 1.3; K329A, 1.2; D333A, 1.2; V335A, 1.5; T336A, 1.4. *C*, four mutants exhibited R*-catalyzed nucleotide exchange rates that were reduced ~3–4-fold relative to the wild-type rate. The estimated values for $t_{1/2}$ were: F330A, 4.1; V331A, 3.2; D337A, 4.6; I338A, 4.0.

F332A, and T325A, were capable of binding GDP and GTPγS and could be activated by GDP/AlF_4^- (Fig. 1*A* and data not shown). In addition, the typical band patterns of trypsin digestion were observed with all of the mutants (Fig. 1*A* and data not shown). These results indicate that the mutations did not disrupt the overall folding of the mutant proteins.

The equivalents of residues Val-328 and Phe-332 are highly conserved not only in Gα subunits, but also among small monomeric G proteins of the Ras superfamily (32). When the equivalent of Phe-332 was replaced with leucine in Ras, the F156L mutant was found to have transforming properties *in vivo* and to accelerate greatly the rate of nucleotide exchange *in vitro* (33). NMR structural studies of Ras F156L revealed alterations in secondary structures α1, α5, and β1–β3 near position 156. The mutation did not appear to reduce the stability of the protein, perhaps due to induction of new intramolecular contacts not present in the wild-type protein. This observation suggests that $G\alpha_t$ F332A might exhibit higher stability than wild-type $G\alpha_t$ in the absence of bound nucleotide.

Because the mutagenesis studies indicate that perturbation of residues in the α5 helix in $G\alpha_t$ causes a dramatic increase in the nucleotide exchange rate, one would predict the existence of intramolecular contacts that maintain the α5 helix in a specific rigid conformation to avoid inappropriate release of GDP. In fact, mutation of residues in the protein core that interact with the α5 helix also resulted in moderate increases in the basal nucleotide exchange rate (Fig. 3*C*). In particular, introduction of alanine at positions Gln-168, Phe-185, Lys-188, or Phe-192 led to increases in nucleotide exchange rate (Table I and data not shown). Gln-168, which is located on αF of the helical domain, hydrogen bonds with the main chain carbonyl of Thr-323. Lys-188, which extends from a loop between β2 and β3, appears to form ionic interactions with two aspartic acid residues on the α5 helix, Asp-333 and Asp-337. These interactions likely serve to maintain the proper register of the α5 helix with respect to the rest of the protein. Phe-185 and Phe-192, which are located on β2 and β3, respectively, are part of a phenylalanine cluster that lies adjacent to Phe-332. These contacts may serve to stabilize the local tertiary structure near the α5 helix, to sense alterations in the position of Phe-332, and to communicate structural changes onto the nucleotide-binding pocket. This latter role is suggested by the structural changes observed in β2 and β3 in NMR studies of the F156L mutant in Ras (33).

It has been proposed previously that interactions between the carboxyl-terminal region of the α5 helix and the rest of the protein were involved in controlling the rate of basal (and possibly R*-catalyzed) nucleotide exchange (34–36). We suggest that these contacts, like those discussed above, stabilize the position of residues in the amino terminus of α5 relative to the rest of $G\alpha_t$. Weakening these contacts, as in the I339A mutant, moderately accelerated nucleotide exchange (Table I), in agreement with previous results (36). However, the magnitude of increases in GDP release rates resulting from mutations of residues in the carboxyl-terminal region of α5 were very small (~4-fold) compared with the effect of mutations closer to the amino terminus of α5.

The gain of function phenotypes of the T325A, V328A, and F332A mutants appear to mimic the effect of R* binding on $G\alpha_t$ in several key respects: (i) the basal rate of nucleotide exchange

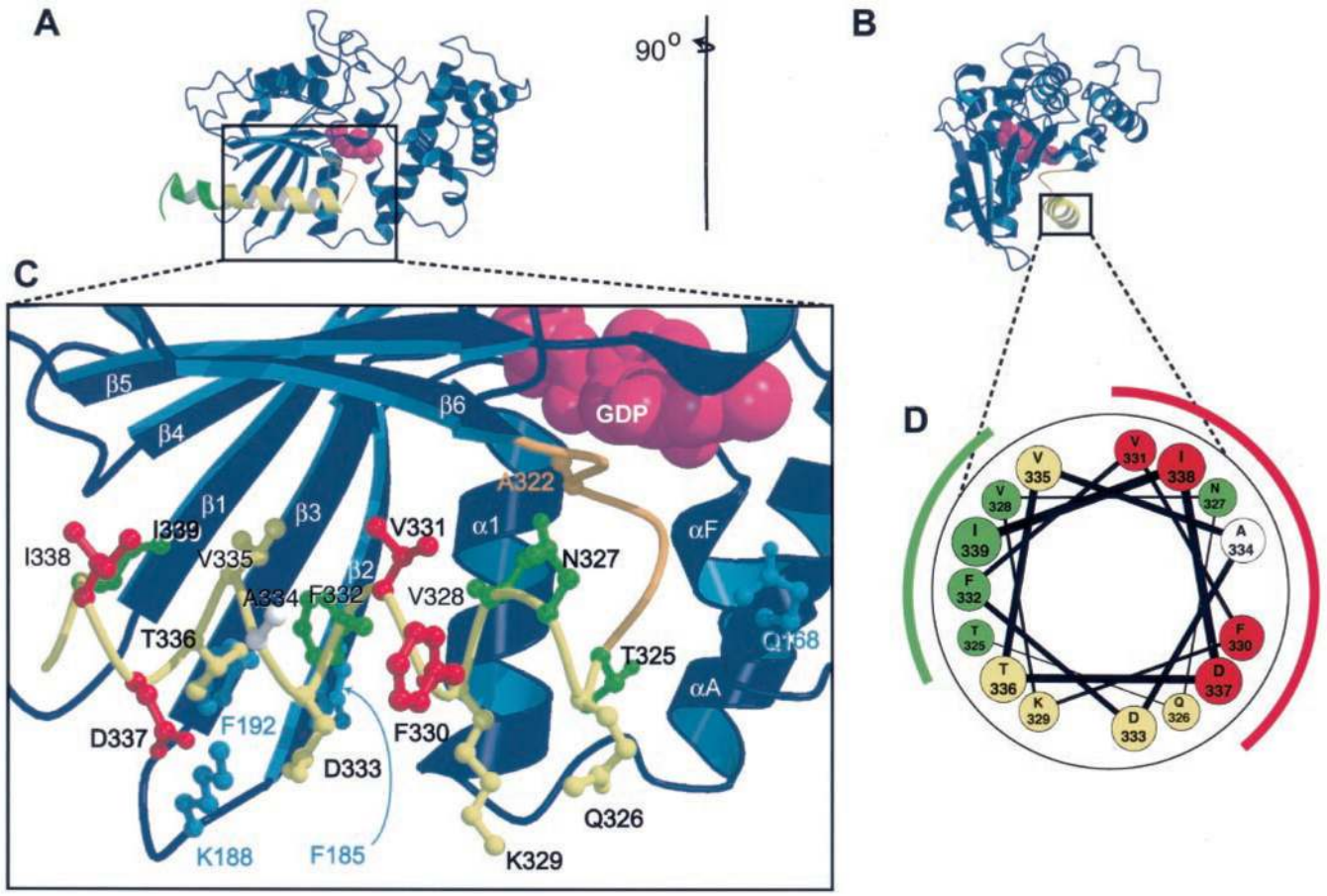

FIG. 3. **The structure of the α5 helix region of $G\alpha_t$ and the effects of site-directed mutations.** *A–C* were prepared with Molscript (43) and Raster3D (44). *A*, structure of the GDP-bound heterotrimeric form of a $G\alpha_t/G\alpha_i$ chimera (PDB entry 1got) (37). The α5 helix (*yellow*) connects the β6/α5 loop (*orange*) with an R*-binding domain, the carboxyl-terminal region (amino acids 340–350) (*green*). The nucleotide is *purple*. The coordinates for the 340–350 region, which are poorly resolved in the crystal structure, were taken from a NMR study of the corresponding peptide in the presence of R* (45) and are not shown in the other panels of this figure. *B*, the molecule has been rotated 90° about a vertical axis relative to *panel A*. The α5 helix is ~50% solvent-exposed and lies in a trough formed by α1 and β1–β6. *C*, close-up view of the α5 region. The residues mutated in this study are shown in *ball-and-stick* representation. Within the α5 helix, residues that led to increases in both basal and R*-catalyzed nucleotide exchange rates when substituted with alanine are colored *green*, residues that led to decreases in R*-catalyzed exchange rate when substituted with alanine are colored *red*, and residues that were indistinguishable from wild-type when substituted with alanine are *yellow*. *D*, helical wheel representation of the α5 helix. The coloring is the same as in *panel C*. The sites of mutations that caused increases in both basal and R*-catalyzed nucleotide exchange map predominantly to a buried surface of the helix. The sites of mutations that caused impairment of R*-catalyzed nucleotide exchange map to a solvent-exposed hydrophobic patch (including Val-331, Ile-338, and Phe-330) adjacent to the buried surface of α5. Hydrophilic residues that map to the "bottom" of the helix did not affect either basal or R*-catalyzed nucleotide exchange when replaced with alanine. Together, the data provide evidence that R* catalyzes nucleotide exchange by perturbing the conformation of residues on the buried surface of α5 (*green line*). These residues communicate with the nucleotide-binding pocket. The perturbation may result from direct binding of R* to the exposed hydrophobic surface of α5 (*red line*).

is tremendously increased, (ii) the primary perturbation is at a distance from the nucleotide-binding site, and (iii) the nucleotide binding properties of the protein are preserved. In principle, perturbation of these residues by R* would be sufficient to catalyze nucleotide exchange.

To explore whether R* actually does induce conformational changes in this region, we measured the R*-catalyzed nucleotide exchange rates in each of the mutants of the α5 helix (Fig. 2). The $G\alpha_t$ mutants that showed the most drastic acceleration of basal nucleotide exchange rates (T325A, V328A, and F332A) could be further stimulated by R* and $G\beta\gamma_t$ (compare Fig. 2*A* with Fig. 1*B*). These mutants displayed faster R*-catalyzed rates than that of wild-type $G\alpha_t$ (Fig. 2*A*), as did N327A and I339A (not shown). These data demonstrate that the T325A, V328A, and F332A mutants could interact with R*. Furthermore, the conformations of the mutant proteins appear to be consistent with or possibly similar to the conformation of R*-bound $G\alpha_t$.

Five mutations caused little or no change in the R*-catalyzed activation rate (Fig. 2*B*). These mutations, Q326A, K329A, D333A, V335A, and T336A, also did not affect the basal nucleotide exchange rate (Table I). Four of these mutations map to the same surface of α5 (Fig. 3*D*); this surface does not appear to be involved in controlling nucleotide exchange rates in $G\alpha_t$.

Four mutants (F330A, V331A, D337A, and I338A) displayed rates of R*-catalyzed activation that were decreased ~3–4-fold relative to the wild-type rate (Fig. 2*C*). Since the mutations did not completely abolish activation by R*, the functions of these residues may be partially redundant. The overall structures of these mutant proteins were not significantly disturbed as indicated by trypsin proteolysis patterns and basal nucleotide exchange rates that were similar to wild-type $G\alpha_t$ (Table I and not shown). The mutations were unlikely to affect interactions with $G\beta\gamma_t$, which is known to bind to the opposite face of $G\alpha_t$ from α5 (37). The most direct interpretation of these loss of function results is that Phe-330, Val-331, Asp-337, and Ile-338 make important contacts in the R*-$G\alpha_t$ complex and that these contacts are disrupted by the substitutions with alanine. In the absence of R*, these residues do not appear to be involved in any contacts that are relevant to nucleotide exchange rates, as

indicated by the crystal structure and the basal nucleotide exchange rates of the corresponding mutants (Fig. 3*C*, Table I). In particular, Phe-330 is more than 4 Å from any other residue. Thus, the formation of important contacts involving Phe-330, Val-331, Asp-337, and Ile-338 in the R*-bound conformation necessitates a R*-induced conformational change in α5. Consistent results were obtained in site-directed spin-labeling studies with $G\alpha_i$, which demonstrated that R*-induced conformational changes occur in a similar set of residues at the amino terminus of α5 corresponding to Gln-326, Asn-327, and Phe-330 of $G\alpha_t$.[2]

Since R* appears to induce conformational changes at Val-331 and Phe-330 and other residues of α5, it is plausible that R* also alters the Thr-325/Val-328/Phe-332 region on the adjacent face of the α5 helix (Fig. 3, *C* and *D*). This is evidence that R* does in fact catalyze nucleotide exchange at a distance by perturbing the Thr-325/Val-328/Phe-332 region and by exploiting the built-in structural connection between these residues and the nucleotide-binding pocket of $G\alpha_t$. Subsequent alteration of the β6/α5 loop as previously hypothesized could also occur (18).

The proposed conformational changes of Thr-325, Val-328, and Phe-332 induced by binding of R* need be only subtle. Because mutation of each residue by itself led to a dramatic increase in nucleotide exchange rate, even a minor structural perturbation of more than one residue simultaneously by R* would be expected to produce a potent effect on the nucleotide exchange rate. As a precedent, the 2.6-Å resolution crystal structure of the $G\alpha_i$ A326S mutant heterotrimer (analogous to A322S in $G\alpha_t$) did not reveal any significant structural alterations although the nucleotide exchange rate was dramatically increased (30).

Some or all of the contacts involving Phe-330, Val-331, Asp-337, and Ile-338 that are inferred to exist in the R*-bound conformation may result from direct binding of R* to α5. The amino acid residues Phe-330, Val-331, Asp-337, and Ile-338 map to a conspicuous solvent-exposed, yet predominantly hydrophobic surface of the α5 helix (Fig. 3). This surface is contiguous with the carboxyl-terminal region (amino acids 340–350), a well documented R*-binding domain. Thus, the exposed surface of α5 may be part of the R*-binding region on $G\alpha_t$, as has been previously suggested (17, 18).

The data are also consistent with the possibility that R* indirectly induces the formation of *intra*molecular contacts involving Phe-330, Val-331, Asp-337, and Ile-338 or a subset thereof. In this scenario, R* would induce changes in the amino terminus of α5 by binding to other sites on the protein, such as the carboxyl-terminal region. As a speculative example, R* might induce a counterclockwise rotation of α5 such that the exposed hydrophobic surface of α5 would become buried, and contacts among Phe-330, Val-331, Asp-337, and Ile-338 would form with the mostly hydrophobic residues in the core of $G\alpha_t$. Such a rotation would of course also displace Thr-325, Val-328, and Phe-332 on the inside surface of α5. Additional experiments are needed to conclusively determine whether the interactions between R* and α5 are direct or indirect.

A number of other proposed mechanisms of R*-catalyzed nucleotide exchange may also be at work. Several studies have suggested that activated receptors might induce opening of the cleft between the Ras-like and helical domains of Gα subunits (8, 38). However, our recent experiments suggest that interdomain interactions are not an energetic barrier to nucleotide exchange in $G\alpha_t$ (24). Others have suggested that R* could use the $G\beta\gamma$ subunits as a lever to distort the Switch I/II regions and facilitate nucleotide exchange (14, 39). This type of mechanism is suggested by analogy to the structure of complexes of monomeric G proteins and their cognate guanine nucleotide exchange factors, in which the guanine nucleotide exchange factors bind to the Switch I and II regions and induce nucleotide dissociation in part by disrupting the Mg^{2+} coordination site of the G protein (14, 40, 41). However, lack of Mg^{2+} in G protein heterotrimers indicates that the monomeric G protein exchange processes cannot be an exact model for the heterotrimeric G proteins (31, 42).

$G\alpha_t$ is a highly specialized molecular switch that exhibits an extremely low rate of basal GDP release and a very rapid rate of R*-catalyzed GTP uptake compared with other G proteins. However, considering the conserved nature of the α5 helix and its orientation to the nucleotide-binding pocket, it is likely that amino acid residues corresponding to Thr-325, Val-328, and Phe-332 in $G\alpha_t$ serve a primary role in regulating nucleotide exchange rate in other Gα subunits.

Acknowledgments—We thank Eugene Simuni and Wing-Yee Fu for assistance with these studies and Prof. Wayne Hubbell (UCLA) for sharing results prior to publication. We especially thank Prof. Henry Bourne (UCSF) for helpful discussions.

[2] W. Hubbell, personal communication.

REFERENCES

1. Bourne, H. R. (1997) *Curr. Opin. Cell Biol.* **9,** 134–142
2. Wess, J. (1997) *FASEB J.* **11,** 346–354
3. Hamm, H. E. (1998) *J. Biol. Chem.* **273,** 669–672
4. He, W., Cowan, C. W., and Wensel, T. G. (1998) *Neuron* **20,** 95–102
5. Berman, D. M., Kozasa, T., and Gilman, A. G. (1996) *J. Biol. Chem.* **271,** 27209–27212
6. Coleman, D. E., Berghuis, A. M., Lee, E., Linder, M. E., Gilman, A. G., and Sprang, S. R. (1994) *Science* **265,** 1405–1412
7. Mixon, M. B., Lee, E., Coleman, D. E., Berghuis, A. M., Gilman, A. G., and Sprang, S. R. (1995) *Science* **20,** 954–960
8. Noel, J. P., Hamm, H. E., and Sigler, P. B. (1993) *Nature* **366,** 654–663
9. Lambright, D. G., Noel, J. P., Hamm, H. E., and Sigler, P. B. (1994) *Nature* **369,** 621–628
10. Tesmer, J. J., Berman, D. M., Gilman, A. G., and Sprang, S. R. (1997) *Cell* **89,** 251–261
11. Slep, K. C., Kercher, M. A., He, W., Cowan, C. W., Wensel, T. G., and Sigler, P. B. (2001) *Nature* **409,** 1071–1077
12. Palczewski, K., Kumasaka, T., Hori, T., Behnke, C. A., Motoshima, H., Fox, B. A., Le Trong, I., Teller, D. C., Okada, T., Stenkamp, R. E., Yamamoto, M., and Miyano, M. (2000) *Science* **289,** 739–745
13. Menon, S. T., Han, M., and Sakmar, T. P. (2001) *Physiol. Rev.* in press
14. Iiri, T., Farfel, Z., and Bourne, H. R. (1998) *Nature* **394,** 35–38
15. Ramdas, L., Disher, R. M., and Wensel, T. G. (1991) *Biochemistry* **30,** 11637–11645
16. Heck, M., and Hofmann, K. P. (2001) *J. Biol. Chem.* **276,** 10000–10009
17. Lichtarge, O., Bourne, H. R., and Cohen, F. E. (1996) *Proc. Natl. Acad. Sci. U. S. A.* **93,** 7507–7511
18. Onrust, R., Herzmark, P., Chi, P., Garcia, P. D., Lichtarge, O., Kingsley, C., and Bourne, H. R. (1997) *Science* **275,** 381–384
19. Hamm, H. E., Deretic, D., Arendt, A., Hargrave, P. A., Koenig, B., and Hofmann, K. P. (1988) *Science* **241,** 832–835
20. Garcia, P. D., Onrust, R., Bell, S. M., Sakmar, T. P., and Bourne, H. R. (1995) *EMBO J.* **14,** 4460–4469
21. Martin, E. L., Rens-Domiano, S., Schatz, P. J., and Hamm, H. E. (1996) *J. Biol. Chem.* **271,** 361–366
22. Osawa, S., and Weiss, E. R. (1995) *J. Biol. Chem.* **270,** 31052–31058
23. Ernst, O. P., Meyer, C. K., Marin, E. P., Henklein, P., Fu, W.-Y., Sakmar, T. P., and Hofmann, K. P. (2000) *J. Biol. Chem.* **275,** 1937–1943
24. Marin, E. P., Gopala Krishna, A., Archambault, V., Simuni, E., Fu, W.-Y., and Sakmar, T. P. (2001) *J. Biol. Chem.* **276,** 23873–23880
25. Sakmar, T. P., and Khorana, H. G. (1988) *Nucleic Acids Res.* **16,** 6361–6372
26. Skiba, N. P., Bae, H., and Hamm, H. E. (1996) *J. Biol. Chem.* **271,** 413–424
27. Min, K. C., Gravina, S. A., and Sakmar, T. P. (2000) *Protein Expression Purif.* **20,** 514–526
28. Fung, B. K., and Nash, C. R. (1983) *J. Biol. Chem.* **258,** 10503–10510
29. Iiri, T., Herzmark, P., Nakamoto, J. M., van Dop, C., and Bourne, H. R. (1994) *Nature* **371,** 164–168
30. Posner, B. A., Mixon, M. B., Wall, M. A., Sprang, S. R., and Gilman, A. G. (1998) *J. Biol. Chem.* **273,** 21752–21758
31. Sprang, S. R. (1997) *Annu. Rev. Biochem.* **66,** 639–678
32. Valencia, A., Chardin, P., Wittinghofer, A., and Sander, C. (1991) *Biochemistry* **30,** 4637–4648
33. Quilliam, L. A., Zhong, S., Rabun, K. M., Carpenter, J. W., South, T. L., Der, C. J., and Campbell-Burk, S. (1995) *Proc. Natl. Acad. Sci. U. S. A.* **92,** 1272–1276
34. Denker, B. M., Schmidt, C. J., and Neer, E. J. (1992) *J. Biol. Chem.* **267,** 9998–10002
35. Denker, B. M., Boutin, P. M., and Neer, E. J. (1995) *Biochemistry* **34,** 5544–5553
36. Muradov, K. G., and Artemyev, N. O. (2000) *Biochemistry* **39,** 3937–3942

37. Lambright, D. G., Sondek, J., Bohm, A., Skiba, N. P., Hamm, H. E., and Sigler, P. B. (1996) *Nature* **379,** 311–319
38. Marsh, S. R., Grishina, G., Wilson, P. T., and Berlot, C. H. (1998) *Mol. Pharmacol.* **53,** 981–990
39. Bohm, A., Gaudet, R., and Sigler, P. B. (1997) *Curr. Opin. Biotechnol.* **8,** 480–487
40. Boriack-Sjodin, P. A., Margarit, S. M., Bar-Sagi, D., and Kuriyan, J. (1998) *Nature* **394,** 337–343
41. Worthylake, D. K., Rossman, K. L., and Sondek, J. (2000) *Nature* **408,** 682–688
42. Sprang, S. R., and Coleman, D. E. (1998) *Cell* **95,** 155–158
43. Kraulis, P. J. (1991) *J. Appl. Crystallogr.* **24,** 946–950
44. Merritt, E. A., and Bacon, D. J. (1997) *Methods Enzymol.* **277,** 505–524
45. Kisselev, O. G., Kao, J., Ponder, J. W., Fann, Y. C., Gautam, N., and Marshall, G. R. (1998) *Proc. Natl. Acad. Sci. U. S. A.* **95,** 4270–4275